

SOFT X-RAY EMISSION LINES IN THE EARLY AFTERGLOW OF GAMMA-RAY BURSTS

DAVIDE LAZZATI, ENRICO RAMIREZ-RUIZ AND MARTIN J. REES
 Institute of Astronomy, University of Cambridge, Madingley Road, Cambridge CB3 0HA, England
 lazzati@ast.cam.ac.uk

Draft version November 2, 2018

ABSTRACT

We compute the luminosity of K_α emission lines produced by astrophysically abundant elements in the soft X-ray spectra of the early afterglow of gamma-ray bursts. We find that the detection of these lines can be a diagnostic for the geometrical set-up of the reprocessing material. In particular we can distinguish between a “geometry dominated” model, in which the line emission is coming from an extended region and its duration arises from light-travel-time effects and an “engine dominated” model, where the line emitting gas is in a smaller region, irradiated for a longer period. These lines therefore offer clues to the dynamics and time-scale of the explosion leading to a gamma-ray burst.

Subject headings: gamma rays: bursts — line: formation — radiation mechanisms: non-thermal

1. INTRODUCTION

Narrow emission features superimposed on the early X-ray afterglow of gamma-ray bursts (GRBs) seem to be common [Piro et al. 1999, Antonelli et al. 2000, Piro et al. 2000 (hereafter P00), Reeves et al. 2002 (hereafter R02)], even though a single strong evidence of their significance is still lacking. These features are observed starting from several hours after the burst (due to instrumental limitations) up to a couple of days. Some have signs of variability (e.g. R02), others are constant for the total duration of the observation (Antonelli et al. 2000; P00). Understanding how and where they are produced is fundamental for identifying the nature of the burst progenitor. In fact the line, being observed at its rest wavelength, has to be produced through reprocessing of the burst radiation, and carries therefore information about the geometry and structure of the material surrounding the burst (Lazzati, Campana & Ghisellini 1999). It is commonly accepted that the presence of metal lines itself strongly favors hypernova models (Woosley 1993; Paczynski 1998) and can be used to rule out compact mergers (Eichler et al. 1989) as burst progenitors. Nevertheless, whether the lines can be produced in a standard hypernova scenario or require an explosive event or supernova that occurred prior to the GRB (see e.g. Vietri & Stella 1998) is still a matter of open debate.

We define as Engine Dominated (ED) the models in which the lines are produced in a standard – single step – hypernova explosion. In these models, the line is created by reprocessing from material very close to the explosion site ($R \sim 10^{13}$ cm). The ionizing continuum in this case can not be attributed to the burst or afterglow itself, since the photons are radiated at larger distances. The ionizing continuum is then believed to be provided by a long lasting engine (Rees & Mészáros 2000) or by magnetic energy stored in a plasma bubble emerging after the jet has crossed the stellar progenitor (Mészáros & Rees 2001). In ED models the duration of line emission is related to the duration of the ionizing continuum.

We define as Geometry Dominated (GD) the models in which the reprocessing material is located at a large enough distance, R , to be illuminated by the burst and afterglow photons. In these models the duration of the line emission is set by the size of the reprocessor. This reprocessing material has to be com-

pact and metal enriched, similar to a supernova remnant (SNR), as naturally predicted in the supernova model (Vietri & Stella 1998). In both ED and GD models the line is supposed to be produced by reflection off a slab of optically thick material (see also Böttcher 2000 and Böttcher & Fryer 2001 for an alternative GD model).

In this letter we compute the luminosity of K_α lines from the elements O, Ne, Mg, Si, S, Ar and Ca (which we will refer to as “light elements” hereafter), and compare them to the iron one. We find that the detection of soft X-ray ($\sim [0.5 - 5]$ keV) features, possibly made in the afterglow of GRB 011211 (R02) strongly favors GD scenarios for the production of metal lines in GRB afterglows. The letter is organized as follows. In §2 we compute the line luminosities in reflection from an *a priori* point of view. We compute the line flux in GD and ED scenario in §3 and we discuss the comparison of predictions with observational constraints in §4.

2. LINE LUMINOSITIES

The luminosity of the lines has been computed according to the equation:

$$L_X = \frac{n_X \epsilon_X S \lambda}{t_{\text{em}}} \quad (1)$$

where the subscript X indicates the particular ion, n_X is the ion density, ϵ_X is the K_α emission line frequency $\epsilon_X = h\nu_X$ of the H-like ion, S is the emitting surface, λ is the depth of the emitting layer and t_{em} is the time scale of emission of a photon by a single ion.

The time scale of photon emission t_{em} can be set either by the ionization time scale corrected for the Auger effect (if the ionization parameter is low) or by the recombination time scale, for highly ionized plasma. Here, we compute the emission time as $\max(t_{\text{rec}}, t_{\text{ion}}/Au_{\{X,Z\}})$, where $Au_{\{X,Z\}}$ is the photoelectric yield for the element X with charge Z (Kaastra & Mewe 1993). The ionization time scale t_{ion} is computed as (Lazzati et al. 2001b):

$$t_{\text{ion}} = (3 + \alpha) \frac{4\pi R^2 h\nu_X^\alpha}{L_0 \sigma_X} \quad (2)$$

where $L(\nu) = L_0 \nu^{-\alpha}$ is the ionizing spectrum (note that L_0 does not have the dimensions of a luminosity), σ_X the threshold cross

section of the element X (atomic data are taken from Verner & Yakovlev 1995) and R the distance of the reprocessing material from the ionizing flux source. The recombination time scale t_{rec} has been computed with the analytic approximations and tables of Verner & Ferland (1996). A constant temperature $T = 4 \times 10^7$ K has been assumed. Both the ionization and recombination time scales are computed for the H-like ion. The charge of the atom is then computed as¹ $Z_X = (t_{\text{ion}}/t_{\text{rec}})^{2/5}$.

The depth of the emitting layer λ is assumed to be the depth that the ionizing photons can reach and/or a line photon can escape without a shift in frequency. We therefore compute it as the minimum between the plasma opacity at resonance for the ion X and the maximum Thompson depth a photon can travel before being shifted by Thomson scattering. We therefore have $\lambda = \min(\lambda_T, \lambda_X)$, where:

$$\lambda_X = \left[\sum_Y \frac{n_Y t_{\{\text{ion}, Y\}} \sigma_Y(\nu_X)}{t_{\{\text{ion}, Y\}} + t_{\{\text{rec}, Y\}}} \right]^{-1} \quad (3)$$

and

$$\lambda_T = \frac{\sqrt{N_{\text{sc}}(T)}}{n_e \sigma_T} \quad (4)$$

where the sum in Eq. 3 is extended over the astrophysically relevant elements H, He, C, N, O, Ne, Mg, Si, S, Ar, Ca, Fe (elemental abundances taken from Anders & Grevesse 1989), and $\sigma_Y(\nu_X)$ is the cross section of element Y computed at the threshold frequency of element X . In the numerator of Eq. 4, $N_{\text{sc}}(T)$ is the maximum number of scatterings a photon can make before the line is smeared or shifted. If $\epsilon \sim kT$, line broadening is more important than shifting, and we have $\sigma_\epsilon/\epsilon \sim \sqrt{kT/(m_e c^2)}$ for a single scattering. Requiring a limit of $\sigma_\epsilon/\epsilon \leq 1/3$ in order for the line to be detectable as a narrow feature, we have $\tau_{\text{max}} = \sqrt{N_{\text{sc}}} \sim [m_e c^2/(9kT)]^{1/2} \approx 4$. Note however that, for the considered abundant elements, Eq. 4 is relevant only for very high ionization parameters (i.e. in the decreasing tails of Fig. 1) and therefore its uncertainty is not necessarily reflected in the maximum efficiency of line reprocessing.

In Fig. 1 and 2 (lower panel) we show the results of our calculations for O, Ne, Mg, Si, S, Ar, Ca and Fe as a function of the ionization parameter $\xi = 4\pi F_{[1-10]}/n$, where $F_{[1-10]}$ is the ionizing flux in the energy range [1-10] keV and n the particle density. The figures show that, in optimal conditions, $\sim 1\%$ of the ionizing flux is reprocessed in each line. We also show that increasing the metallicity does not increase this fraction, but helps keep it constant for high ionization parameters. The accuracy of this line strength estimates have been checked against the results of numerical simulations for Mg, Si and Fe (Ross 1979; Ross & Fabian 1983; Ballantyne, Fabian & Ross 2002). We find that our results are in agreement within a factor ~ 2 with line luminosities obtained by fitting Gaussian profiles to the numerical spectra. The largest deviations are observed close to the minimum value of the efficiency (in the strong Auger regime), where our semi-analytical approach yields larger luminosities with respect to the full numerical treatment. This comparison has been performed with Mg, Si and Fe lines, since the numerical code does not include S, Ar and Ca.

3. GRB MODELS

In order to apply the results of the previous section to various GRB models, we need to transform the ratios shown in Fig. 1 and 2 into observed fluxes and/or luminosities. Even though in spectroscopy it is customary to compute the line equivalent width, in the case of GRBs it is assumed that the observed continuum is not related to the ionizing continuum responsible for producing the lines (which can be the afterglow itself at earlier times in GD models or a completely different component in ED models), and so it is more useful to directly compare the line fluxes (Lazzati et al. 1999).

3.1. Geometry dominated models

In the case of GD models, the observed line flux has to be corrected by a geometric factor ζ . This factor takes into account that while the emitting material is illuminated for a time t_{ill} , the line is observed, at infinity, for a time $t_{\text{obs}} \sim R_{\text{SNR}}/c$. A precise computation of $\zeta \equiv t_{\text{ill}}/t_{\text{obs}}$ is complex, since the reprocessing material is illuminated by the burst and early afterglow radiation, and it is likely that the properties of the fireball towards the reprocessing material are different from those along the line of sight (Rossi, Lazzati & Rees 2002). If one assumes that the fireball decelerates inside the remnant and that the density of the external medium in the immediate vicinity of the progenitor scales with the remnant radius² as $n = 10^8 n_8 (R_{\text{SNR}}/10^{15})^{-3} \text{ cm}^{-3}$, the time the fireball takes to overtake the remnant is proportional to the radius of the remnant itself, and:

$$\zeta \sim \frac{c(t_{\text{GRB}} + t_{\text{ill}})}{R_{\text{SNR}}} \approx \frac{c t_{\text{ill}}}{R_{\text{SNR}}} \approx 0.05 \frac{n_8}{E_{51}} \quad (5)$$

where t_{GRB} is the burst duration, and E_{51} is the isotropic equivalent energy output of the burst in units of 10^{51} erg in the direction of the reprocessing material. We have used Eq. 15 of Panaitescu & Kumar (2000) to evaluate the numerical factor.

On the other hand, in GD models the ionizing continuum is not directly observed, and can then be assumed to be much larger than the afterglow luminosity at the time the line is detected. The ratio η_{cont} of reflected to incident continuum depends on the ionization parameter, ranging from < 0.1 for $\xi \leq 10^2$ to ~ 1 for $\xi \geq 10^5$ (see the upper panel of Fig. 2). For reasonable ionization parameters, one can then assume an ionizing luminosity $L_{\text{ion}} \leq L_{\text{After}}/(\zeta \eta_{\text{cont}}) \sim 2 \times 10^{48} \text{ erg s}^{-1}$, where L_{After} is the afterglow [1-10] keV luminosity at the time at which the lines are observed. The apparent contradiction of having an ionizing continuum brighter than the afterglow but not observed in the afterglow itself, is solved if we consider the geometry of the system (see e.g. panels a and b of Fig. 2 in Vietri et al. 2001). In fact, the fireball emission towards the reprocessing material is not necessarily related to the one in the direction of the observer. Moreover, line photons produced at time t are observed at a later time due to the longer travel they have to make. At this later time the afterglow emission has decreased.

Finally, we must take into account that while the ionizing continuum may be geometrically beamed, the line emission is nearly isotropic, so that the observed flux must be corrected by a factor $\Omega/4\pi \sim 0.25$, where the numerical factor has been computed for a jet opening angle of $\theta = 40^\circ$. This opening angle is one order of magnitude larger than the opening

¹The exponent 2/5 has been derived by interpolation of the numerical recombination rates of Shull & van Steenberg (1982).

²Note that the density is not supposed to scale with the radius. We consider a uniform density inside the remnant, scaling it with the remnant radius in order to have a constant total mass inside it.

angle measured in GRB 991216 (Frail et al. 2001). Since $\Omega/4\pi = 1 - \cos\theta_j \propto \theta_j^2$, a ten times smaller opening angle would make the lines two orders of magnitude fainter and thus undetectable. We here assume this larger angle without discussing its implications, referring the reader to the thorough discussion presented in Ghisellini et al. (2002).

The resulting line luminosity of the element X is then given by:

$$L_X = \frac{\Omega}{4\pi} \zeta L_{\text{ion}} \eta_X \sim 0.25 \frac{\eta_X}{\eta_{\text{cont}}} L_{\text{After}} \quad (6)$$

where η_X is the luminosity ratio plotted in Fig. 1. Note that the geometric factor ζ is not relevant in this expression. For low ionization parameters $\xi < 10^3$ one has $\eta_{\text{cont}} \sim 0.1$ and $\eta_X \sim 10^{-2}$, while for iron one obtains $\eta_{\text{Fe}} \sim 10^{-3}$ since its efficiency is strongly decreased by Auger auto ionization (see also Ross, Fabian & Brandt 1996). Light elements can reprocess into K_α line emission a sizable fraction of the continuum, yielding luminosities of the order of $L_X \sim 2.5 \times 10^{44}$ erg s⁻¹ ($F_X \sim 5 \times 10^{-14}$ erg cm⁻² s⁻¹ at $z \sim 1$). In contrast, iron K_α emission will be one order of magnitude fainter, and therefore undetectable with present instrumentation. For larger ionization parameters $10^3 < \xi < 10^4$, iron emission is efficient, while light elements are too ionized to emit line photons. A bright iron line should then be detectable in absence of light element features (see also Ballantyne & Ramirez-Ruiz 2001).

3.2. Engine dominated models

Evaluating the line luminosity in ED models is simpler and less affected by uncertainties. In fact, there is no geometric dilution of the photons and the ionizing continuum is likely to be smaller than the afterglow luminosity at the time of the line observation. Only the beaming factor $\Omega/4\pi$ has to be taken into account, yielding a luminosity:

$$L_X = \frac{\Omega}{4\pi} L_{\text{After}} \eta_X \sim 0.25 L_{\text{After}} \eta_X \quad (7)$$

In ED models, then, the line luminosity is a factor η_{cont} less intense than in GD models. Lines from light elements (Mg, Si, S, Ar and Ca), should be very difficult to detect since $L_{\{\text{Ar,Ca}\}} \leq 10^{43}$ erg s⁻¹ ($F_X \sim 10^{-15}$ erg cm⁻² s⁻¹ at $z \sim 1$). Iron lines should instead be detectable, in particular if the ionization is not too high and the spectral slope is flat (Ballantyne et al. 2002).

4. SUMMARY AND DISCUSSION

The presence of emission features in the early X-ray afterglows of GRBs provides important clues for identifying the burst progenitor. We computed the luminosity of K_α emission features from astrophysically relevant elements (Mg, Si, S, Ar and Ca) in reflection models and applied the results to the detectability of those features in the early afterglows of GRBs. We find that the line luminosity of these elements can be a strong indicator of the geometry of the reprocessing material. In particular, light element lines are detectable only if the ionizing continuum is not directly observable. This geometrical set-up is naturally accounted for in GD models, in which the line photons reach the observer after being reflected by material away from the line of sight. In ED models, the ionizing continuum and the line are observed simultaneously and for this reason the strength of light elements lines is greatly diluted, making them undetectable.

Recently, a possible detection of K_α emission lines from light elements in the early afterglow of GRB 011211 has been claimed (R02). Reeves et al. claim that their spectrum is inconsistent with a reflection model. We should however be aware that the reflection model used to fit the data does not include emission from S, Ar and Ca (Ross & Fabian 1983). In addition, they fit a pure reflection model, without including the power-law external shock emission. This power-law component must however dominate the continuum, since the broad band lightcurve decreases as a power-law in time (R02). Let us now consider the K_α line of sulphur at 2.6 keV. It is detected at a flux level of $(1 \pm 0.3) \times 10^{-14}$ erg cm⁻² s⁻¹, when the [0.2-10] keV continuum has a flux of $\sim 2 \times 10^{-13}$ erg cm⁻² s⁻¹. This flux ratio $\eta_S = 0.05 \pm 0.015$ can be compared to the lower left panel of Fig. 1 and Eq. 7. Even if the beaming correction approaches unity, the detected flux ratio exceeds the maximum allowed in an ED model, regardless of both the value of the spectral slope and ionization parameter. In GD models, however, the luminosity of light element features can be ten times larger due to the very small fraction of the continuum that is reflected for small ionization parameters (see the upper panel of Fig. 2).

Another important particularity of the observation of light element features in GRB 011211 is the lack of an iron line. If we compare this observation to that of the iron K_α line in GRB 991216 (P00), we find that the ratio of iron to sulphur luminosities is significantly different. The line ratio is $L_S/L_{\text{Fe}} < 0.4$ in GRB 991216 and $L_S/L_{\text{Fe}} > 2$ in GRB 011211. This difference can be explained, as a consequence of the different ionization state of the reprocessing material – in GRB 011211 the reprocessing material had an ionization parameter between $30 \leq \xi \leq 300$, while in GRB 991216 $10^3 < \xi < 10^5$. In the framework of GD models, the different ionization parameter can be interpreted as a different age of the SNR at the time of the burst explosion. If the remnant itself has a density that scales with the radius (and hence with age) $n_{\text{SNR}} \propto R_{\text{SNR}}^{-3}$, the ionization parameter should also scale with radius for a constant ionizing luminosity. Young remnants should then produce light element lines, possibly in coincidence with weak nickel and/or cobalt lines, while old remnants should produce high ionization iron lines, and no light element features (see also Vietri et al. 2001). In addition, the variability time scale of compact remnants should be smaller. All these predictions are confirmed by observations – the features observed in GRB 011211, in which a marginal evidence of Ni line is present, are observed to disappear after ~ 4 h (R02), while the iron line in GRB 991216 is detected ~ 18 h after the burst (P00). It should also be remarked that these conclusions do not depend on the assumption of a constant temperature of the reprocessing material. In fact, should this assumption be wrong or the temperature be estimated incorrectly, the result would be an horizontal shift of the lines in Fig. 1. Since we have not discussed in which conditions a certain value of the ionization parameter is relevant, this does not affect the generality of our conclusions.

In conclusion, the detection of Mg, Si, S, Ar and Ca lines with equivalent widths of hundreds of eV in the early afterglow of GRB 011211 can not be accounted for in any version of ED models. A two step explosion is necessary, in order to place the reprocessing material at a distance large enough to explain the duration of the line and to let the ionizing continuum fade (hidden by the afterglow emission) before the lines can be observed. This evidence adds to the transient absorption feature detected in GRB 990705 (Amati et al. 2000; Lazzati et al.

2001a) which strongly favors a GD model. Alternatively, the reflecting material may have been expelled during the common envelope phase of a binary progenitor system composed by a compact object and a helium star (Böttcher & Fryer 2001). In this case, all the discussion about GD models hold true, but a Ni line is not expected since the reprocessing material is not a SN explosion.

We are very grateful to K. Pounds and J. Reeves for useful discussions on the data of GRB 011211 and to A. Fabian and D. Ballantyne for many discussions on reflection spectra, and for making their numerical spectra available to us. We thank Markus Böttcher for useful discussions.

REFERENCES

- Amati, L. et al. 2000, *Science*, 290, 953
 Anders, E. & Grevesse, N., 1989, *Geochimica et Cosmochimica Acta* 53, 197
 Antonelli, L. A. et al. 2000, *ApJ*, 545, L39
 Ballantyne, D. R. & Ramirez-Ruiz, E. 2001, *ApJ*, 559, L83
 Ballantyne, D. R. , Ramirez-Ruiz, E., Lazzati, D. & Piro, L. 2002, submitted to *A&A*
 Ballantyne, D. R., Fabian, A. C., & Ross, R. R. 2002, *MNRAS*, 329, L67
 Böttcher, M. 2000, *ApJ*, 539, 102
 Böttcher, M. & Fryer, C. L. 2001, *ApJ*, 547, 338
 Eichler, D., Livio, M., Piran, T., & Schramm, D. N. 1989, *Nature*, 340, 126
 Frail, D. A. et al. 2001, *ApJ*, 562, L55
 Ghisellini, G., Lazzati, D., Rossi, E., & Rees, M. J. 2002, *A&A* submitted
 Kaastra, J. S. & Mewe, R. 1993, *A&AS*, 97, 443
 Lazzati, D., Campana, S., & Ghisellini, G. 1999, *MNRAS*, 304, L31
 Lazzati, D., Ghisellini, G., Amati, L., Frontera, F., Vietri, M., & Stella, L. 2001a, *ApJ*, 556, 471
 Lazzati, D., Perna, R. & Ghisellini, G. 2001b, *MNRAS*, 325, L19
 Mészáros, P. & Rees, M. J. 2001, *ApJ*, 556, L37
 Paczynski, B. 1998, *ApJ*, 494, L45
 Panaitescu, A. & Kumar, P. 2000, *ApJ*, 543, 66
 Piro, L. et al. 1999, *ApJ*, 514, L73
 Piro, L. et al. 2000, *Science*, 290, 955 (P00)
 Reeves, J. N., et al. 2002, *Nature*, 416, 512 (R02)
 Rees, M. J. & Mészáros, P. 2000, *ApJ*, 545, L73
 Ross, R. R. 1979, *ApJ*, 233, 334
 Ross, R. R. & Fabian, A. C. 1993, *MNRAS*, 261, 74
 Ross, R. R., Fabian, A. C. & Brandt, W. N. 1996, *MNRAS*, 278, 1082
 Rossi, E., Lazzati, D. & Rees, M. J. 2002, *MNRAS*, 332, 945
 Shull, J. M. & van Steenberg, M. 1982, *ApJS*, 48, 95
 Verner, D. A. & Yakovlev, D. G. 1995, *A&AS*, 109, 125
 Verner, D. A. & Ferland, G. J. 1996, *ApJS*, 103, 467
 Vietri, M. & Stella, L. 1998, *ApJ*, 507, L45
 Vietri, M., Ghisellini, G., Lazzati, D., Fiore, F., & Stella, L. 2001, *ApJ*, 550, L43
 Woosley, S. E. 1993, *ApJ*, 405, 273

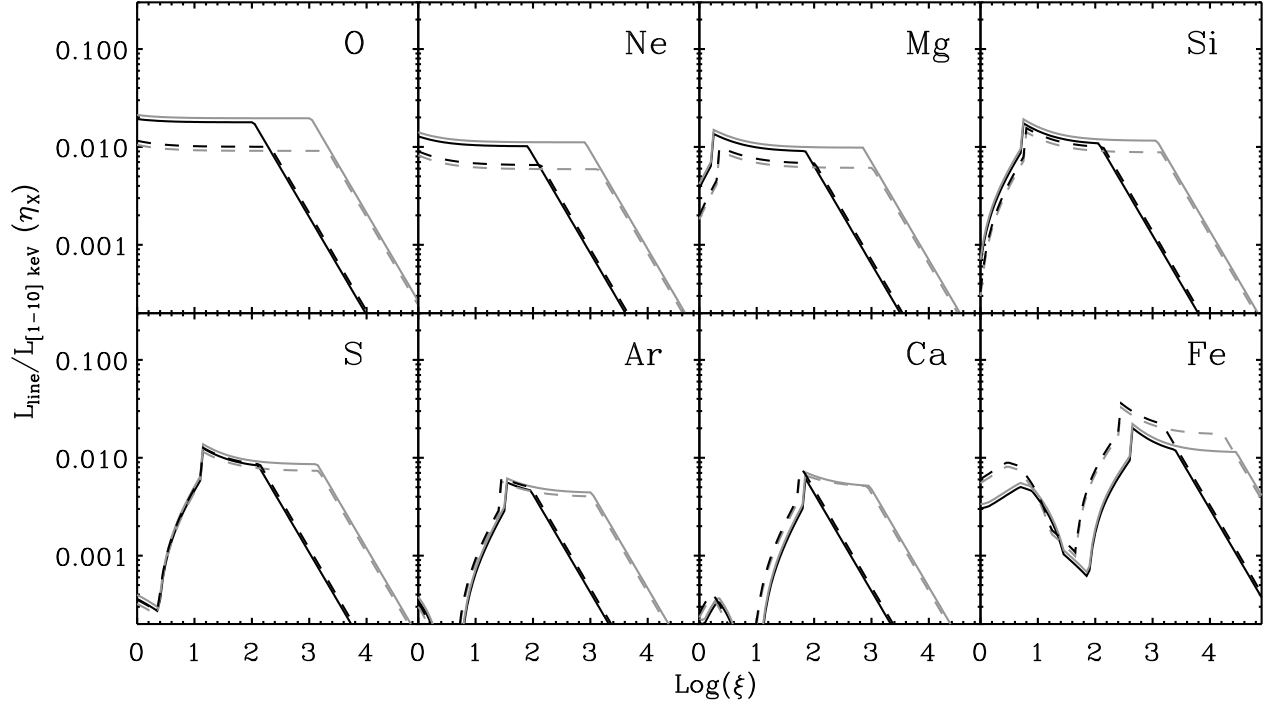


Fig. 1.— Ratio of the K_α line to the [1-10] keV continuum luminosities for various astrophysically relevant elements as a function of the ionization parameter $\xi \equiv 4\pi F_{[1-10]}/n$. Solid and dashed lines correspond to a power-law index $\alpha = 1.25$ and $\alpha = 0.75$ of the ionizing continuum, respectively. Black and grey lines correspond to solar and ten times solar metallicity of the reprocessing material, respectively.

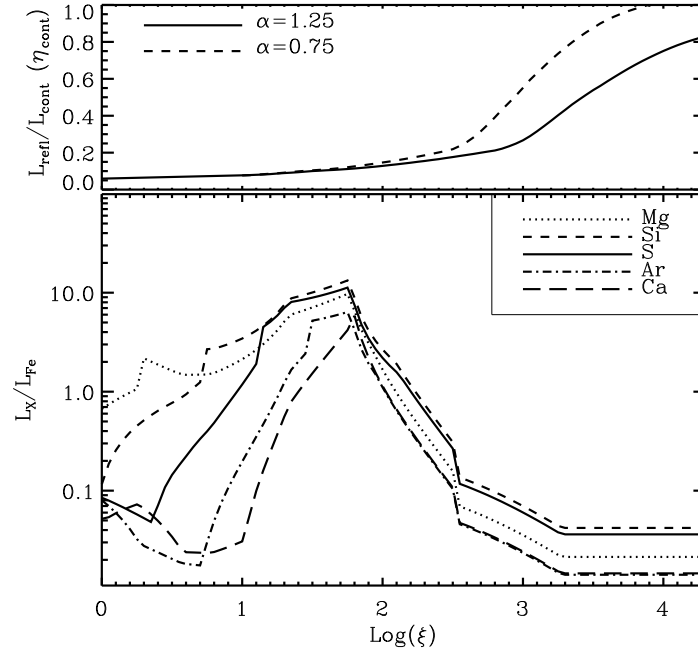


Fig. 2.— Upper panel: ratio of the reflected to incident continuum in the [1-10] keV band for a solar metallicity slab. Two incident spectral slopes are considered, as in Fig. 1. Lower panel: ratio of K_α line luminosities of Mg, Si, S, Ar and Ca to the iron K_α luminosity. Even though the iron line is generally more intense than all the other lines, there is a range of ionization parameters $\xi \sim 10^2$ for which iron K_α emission is quenched by Auger auto ionization, and light elements dominate. This figure is made for a continuum power-law index $\alpha = 1.0$ and solar metallicity. Changing these parameters can be a moderate effect on the shape of the curves (see Fig. 1).